ISSN 1674-1056
http://cpb.iphy.ac.cn
http://iopscience.iop.org/cpb
中国物理 B
Chinese Physics
中国物理 Chinese Physics B

Light-shift induced by two unbalanced spontaneous decay rates in EIT (CPT) spectroscopies under Ramsey pulse excitation

Xiaoyan Liu(刘晓艳), Xu Zhao(赵旭), Jianfang Sun(孙剑芳), Zhen Xu(徐震), and Zhengfeng Hu(胡正峰)
Citation: Chin. Phys. B, 2021, 30 (**8**): 083203. DOI: 10.1088/1674-1056/ac0528
Journal homepage: http://cpb.iphy.ac.cn; http://iopscience.iop.org/cpb

What follows is a list of articles you may be interested in

An effective pumping method for increasing atomic utilization in a compact cold atom clock

Xin-Chuan Ouyang(欧阳鑫川), Bo-Wen Yang(杨博文), Jian-Liao Deng(邓见辽), Jin-Yin Wan(万金银), Ling Xiao(肖玲), Hang-Hang Qi(亓航航), Qing-Qing Hu(胡青青), and Hua-Dong Cheng(成华东)
Chin. Phys. B, 2021, 30 (**8**): 083202. DOI: 10.1088/1674-1056/abfccd

High-precision three-dimensional Rydberg atom localization in a four-level atomic system

Hengfei Zhang(张恒飞), Jinpeng Yuan(元晋鹏), Lirong Wang(汪丽蓉), Liantuan Xiao(肖连团), and Suo-tang Jia(贾锁堂)
Chin. Phys. B, 2021, 30 (**5**): 053202. DOI: 10.1088/1674-1056/abd46f

Coherent 420 nm laser beam generated by four-wave mixing in Rb vapor with a single continuous-wave laser

Hao Liu(刘浩), Jin-Peng Yuan(元晋鹏), Li-Rong Wang(汪丽蓉), Lian-Tuan Xiao(肖连团), Suo-Tang Jia(贾锁堂)
Chin. Phys. B, 2020, 29 (**4**): 043203. DOI: 10.1088/1674-1056/ab75d9

Precise measurement of a weak radio frequency electric field using a resonant atomic probe

Liping Hao(郝丽萍), Yongmei Xue(薛咏梅), Jiabei Fan(樊佳蓓), Jingxu Bai(白景旭), Yuechun Jiao(焦月春), Jianming Zhao(赵建明)
Chin. Phys. B, 2020, 29 (**3**): 033201. DOI: 10.1088/1674-1056/ab6c49

Automatic compensation of magnetic field for a rubidium space cold atom clock

Lin Li(李琳), Jingwei Ji(吉经纬), Wei Ren(任伟), Xin Zhao(赵鑫), Xiangkai Peng(彭向凯), Jingfeng Xiang(项静峰), Desheng Lü(吕德胜), Liang Liu(刘亮)
Chin. Phys. B, 2016, 25 (**7**): 073201. DOI: 10.1088/1674-1056/25/7/073201

Light-shift induced by two unbalanced spontaneous decay rates in EIT (CPT) spectroscopies under Ramsey pulse excitation*

Xiaoyan Liu(刘晓艳)[1,2], Xu Zhao(赵旭)[1,3], Jianfang Sun(孙剑芳)[1,2], Zhen Xu(徐震)[1,2,†], and Zhengfeng Hu(胡正峰)[1,2,3,4,‡]

[1] *The Key Laboratory of Quantum Optics, Shanghai Institute of Optics and Fine Mechanics, Chinese Academy of Sciences, Shanghai* 201800, *China*

[2] *Center of Materials Science and Optoelectronics Engineering, University of the Chinese Academy of Sciences, Beijing* 100049, *China*

[3] *Department of Physics, Shanghai University, Shanghai* 200444, *China*

[4] *CAS Center for Excellence in Ultra-intense Laser Science, Shanghai* 201800, *China*

(Received 25 March 2021; revised manuscript received 20 May 2021; accepted manuscript online 26 May 2021)

Light shift is important and inevitably affects the long-term stability of an atomic clock. In this work, considering two unbalanced branches of the spontaneous decay rate in a three-level system, we studied the frequency shifts of electromagnetically induced transparency (EIT) and coherent population trapping (CPT) clocks operating under the pulse sequence regime by numerically solving the Liouville density matrix equations. The results show that the frequency shifts are larger when the two branches of spontaneous emission rate are not equal compared to the equal case. In addition, in EIT-Ramsey, the effect of the unbalanced branches of the spontaneous decay rate and relaxations of low-energy states on the frequency shift is greater than that of Rabi frequency. In CPT-Ramsey, the relaxations of low-energy states play a dominant role in frequency shift.

Keywords: atom clock, light shfit, laser–atom interaction, quantum optics

PACS: 32.70.Jz, 32.80.Qk, 37.10.Jk, 06.20.Jr **DOI:** 10.1088/1674-1056/ac0528

A compact atomic clock is very important to many applications, such as global positioning system (GPS), inertial navigators, distributed networks, and so on.[1] Earlier researches on this type of the frequency standards are based on the interactions between light (microwave) and atoms, such as light–microwave double resonances.[2] Recently, electromagnetically induced transparency (EIT) and coherent population trapping (CPT) have been extensively studied because of their very interesting phenomena.[3–7] One interesting phenomenon is that they have a very narrow spectroscopic line which can be applied to sensitive metrology, such as the use for the frequency standard and optical magnetometry.[8] Especially, they can be used to obtain the clock signal of a compact vapor cell or laser cooling cold ensemble atoms devices. Within the microwave frequency range, due to the absence of microwave cavity, they have been considered to be applied to realistic navigation and movable systems.[9–15] In the optical frequency regime, the EIT (CPT) approach has been used to generate optical atom clock transition signal.[16] It is well known that frequency shift is very important to the long-term stability of a frequency standard. In EIT (CPT)-Ramsey (EIT-Ramsey, CPT-Ramsey) spectroscopy,[17–20] since the lasers are used in a time-separated way and there is a dark zone without lasers interacting with atoms, the frequency shift will be reduced. However, the frequency shift is still affected by the parameters of light fields and atoms, such as the difference between the two branches of the spontaneous decay rate, relaxations of low-energy states, Rabi frequency, etc.[17–19] In an alkali metal three-level atomic system,[21] the populations of the excited state decay into the two low-energy states with equal rates, but in an alkaline-earth metal three-level atomic system,[16] two branches of spontaneous emission rate are different. Besides, there are several differences between the EIT and CPT processes,[22–24] for example, two lasers called coupling and probe lasers with different intensities are applied to the three-level atomic ensemble in the EIT process. Usually the coupling laser is much more intense than the probe laser. As a result, in the atom system, most of the populations stay in the state which interacted with the probe laser. Compared to the EIT process, in a CPT process, the two lasers applied to the atomic system have almost equal intensity. This interaction results in the equal population distribution of the low-energy states for the atoms. Since the two unbalanced branches of the spontaneous decay rate and the two unequal Rabi frequencies will induce the unequal population distributions in the atomic system, the unequal population distributions will induce larger frequency shifts. Therefore, in this work, we closely investigated the frequency shifts under the Ramsey spectroscopies with the different Rabi frequencies, two unbalanced branches of spontaneous rate, as well as the relaxations of atomic low-

*Project supported by the State Key Laboratory of Low Dimensional Quantum Physics Research Program, Tsinghua University (Grant No. KF201707).

†Corresponding author. E-mail: xuzhen@siom.ac.cn

‡Corresponding author. E-mail: zfhu@siom.ac.cn

energy states by strict numerical calculations. On this basis, we further analyzed and compared the influence of these parameters on the frequency shifts in the EIT-Ramsey and CPT-Ramsey processes.

The laser–atom interaction system is shown in Fig. 1. Two lasers are applied to a closed Λ-type three-level atomic system, as shown in Fig. 1(a). $|1\rangle$ is the ground state of an atom, $|2\rangle$ is the ground state for an alkaline atom or the metastable state for an alkaline-earth atom, which can be the clock transition states, and $|3\rangle$ is the excited state. The two lasers drive the transitions from the states $|1\rangle$, $|2\rangle$ to the excited state. We used the density matrix to represent the atomic system, so that the population transfer caused by the spontaneous emission of the excited state and the collision between the low energy states can be naturally included in the density matrix equation. Considering all relaxations and decoherences, the temporal evolution of the light–atom interaction system is given by the liouville density matrix equation

$$\frac{\mathrm{d}}{\mathrm{d}t}\rho = \frac{1}{\mathrm{i}\hbar}[H,\rho] + R\rho, \tag{1}$$

where H is the Hamiltonian of the system and R is the relaxation. Under the rotation wave approximation, the optical Bloch equations can be obtained which describe the temporal evolution of the density matrix,

$$\begin{aligned}
\dot{\rho}_{11} &= (\mathrm{i}\Omega_1\rho_{13} + \mathrm{c.c.}) + \Gamma_{31}\rho_{33} - \gamma(\rho_{11} - \rho_{22}),\\
\dot{\rho}_{22} &= (\mathrm{i}\Omega_2\rho_{23} + \mathrm{c.c.}) + \Gamma_{32}\rho_{33} - \gamma(\rho_{22} - \rho_{11}),\\
\dot{\rho}_{33} &= -(\mathrm{i}\Omega_1\rho_{13} + \mathrm{c.c.}) - (\mathrm{i}\Omega_2\rho_{23} + \mathrm{c.c.}) - \Gamma\rho_{33},\\
\dot{\rho}_{13} &= \mathrm{i}\Omega_1(\rho_{11} - \rho_{33}) + \mathrm{i}\Omega_2\rho_{12} - \left(\frac{\Gamma+\gamma}{2} + \mathrm{i}\Delta_1\right)\rho_{13},\\
\dot{\rho}_{23} &= \mathrm{i}\Omega_2(\rho_{22} - \rho_{33}) + \mathrm{i}\Omega_1\rho_{21} - \left(\frac{\Gamma+\gamma}{2} + \mathrm{i}\Delta_2\right)\rho_{23},\\
\dot{\rho}_{12} &= -\mathrm{i}\Omega_1\rho_{32} + \mathrm{i}\Omega_2\rho_{13} - [\gamma + \mathrm{i}(\Delta_1 - \Delta_2)]\rho_{12},
\end{aligned} \tag{2}$$

where ρ_{ii} $(i = 1, 2, 3)$ correspond to the atomic population, and $\rho_{ji} = \rho_{ij}^*$ $(i, j = 1, 2, 3)$, which correspond to coherence between the atomic states. $\rho_{11} + \rho_{22} + \rho_{33} = 1$ is the population conservation for a closed system. The laser with the Rabi frequency Ω_1 drives the transition between the states $|1\rangle$ and $|3\rangle$. The laser with the Rabi frequency Ω_2 is applied to the transition from the state $|2\rangle$ to the state $|3\rangle$, where the Rabi frequencies Ω_1 and Ω_2 are determined by the product of the electric dipoles in $|1\rangle \leftrightarrow |3\rangle$ transition and $|2\rangle \leftrightarrow |3\rangle$ transition and the electric field amplitudes, respectively. Δ_1 and Δ_2 are the one-photon detunings of the two lasers, respectively. $\Delta_0 = \Delta_1$ is the common optical detuning, $\delta = \Delta_1 - \Delta_2$ is the Raman detuning in the configuration, where the frequency of one laser is fixed while the other laser is frequency scanned. Γ is the decay rate from the excited state to the low energy states, and Γ_{31} and Γ_{32} are the decay rates from the excited state $|3\rangle$ to the states $|1\rangle$ and $|2\rangle$, respectively, which may or may not be the same. γ is the relaxation of the low energy states ($\gamma_1 = \gamma_2 = \gamma$). The density matrix equation completely describes the characteristics of the system, such as transient dynamics, population transition, and quantum coherence between states.

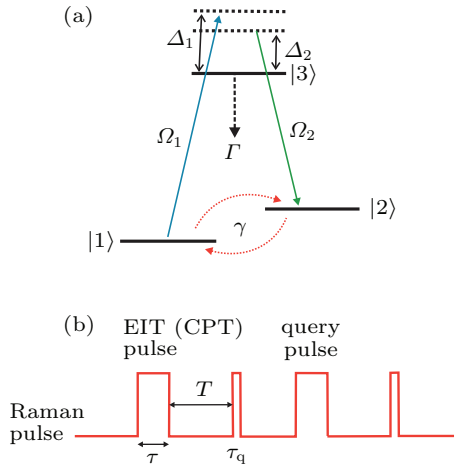

Fig. 1. The laser–atom interacting system for generating Ramsey spectral lines. (a) Diagram for lasers Λ-type atoms interacting and its related transitions. The laser with Rabi frequency Ω_1 and the other laser field with Rabi frequency Ω_2 drive the transitions $|1\rangle \leftrightarrow |3\rangle$ and $|2\rangle \leftrightarrow |3\rangle$, respectively. The decay rate of the excited state to the low energy states is Γ and the relaxation rate of the low energy states is γ. (b) Time sequence for generating Ramsey spectral line. EIT (CPT) laser–atom interacting time is τ and free evolution time is T. The detecting time is τ_q.

For the generation of Ramsey spectrum, the pulse action time sequence is shown in Fig. 1(b). The first laser pulse is CPT (EIT) generation pulse, and its duration τ should be long enough so that the atoms can reach the dark state. The choice of this time is based on the formation of steady state. If the time is short, the steady-state coherence of the low-energy states will not be formed, and the frequency shifts will increase. After coherent preparation, the atoms will undergo free evolution within the duration T. During the free evolution duration, there are no interactions between the lasers and the atoms. In this stage, there is a cumulative phase difference between the atomic coherence and the evolution phase of the Raman field. The line width and frequency shift of the atomic clock transition spectrum are inversely proportional to this time. However, due to relaxations of the atomic states and working environment of the atomic clock, a longer T will reduce the signal-to-noise ratio of the atomic clock transition spectrum. The appropriate free evolution time is usually selected according to the ratio of line width and signal-to-noise ratio. After the free evolution, a short pulse is used to detect Ramsey interference. The longer detection time τ_q will result in the optical re-pumping process and the increase of frequency shift. Since the query pulse is very short, the Ramsey interference fringes detected by the query pulse cannot be studied by steady-state analysis. Therefore, we used accurate numerical calculation on the density matrix equation given by Eq. (2). In the computation process, we used the following initial parameters: $\rho_{11}^0 = 0.6$, $\rho_{22}^0 = 0.4$, $\rho_{33}^0 = \rho_{ij}^0 = 0$ $(i, j = 1, 2,$

3), where ρ_{ii}^0 represents the initial population of states $|1\rangle$, $|2\rangle$, and $|3\rangle$ in turn, and ρ_{ij}^0 represents the initial values of the Raman coherence. Ramsey interference fringes are obtained by repeated calculation for the different δ values around $\delta = 0$. The frequency shift we calculated is the shift of the center fringe.

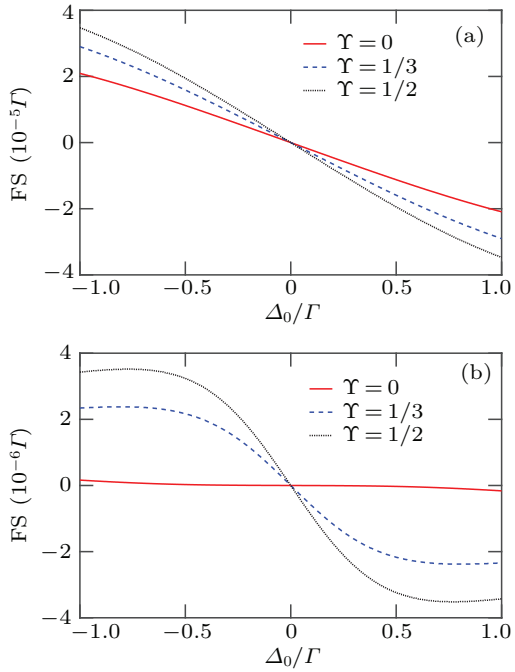

Fig. 2. (a) FSs of the center fringe of the EIT-Ramsey on the ρ_{33} excited state population vs. the common optical detuning Δ_0 with the different normalized branch ratio Υ. The Rabi frequencies are $\Omega_1 = 0.02\Gamma$ and $\Omega_2 = 0.005\Gamma$. The decay rates of the ground state are $\gamma = 1 \times 10^{-4}\Gamma$. The normalized branch ratios are $\Upsilon = 0$ (red soild line), $\Upsilon = 1/3$ (blue dashed line), and $\Upsilon = 1/2$ (black dotted line) respectively. (b) FSs of the center fringe of the CPT-Ramsey on the ρ_{33} excited state population vs. the common optical detuning Δ_0 with the different normalized branch ratio Υ. The Rabi frequencies are $\Omega_1 = \Omega_2 = 0.005\Gamma$. The decay rates of the ground state are $\gamma = 1 \times 10^{-4}\Gamma$. The normalized branch ratios are $\Upsilon = 0$ (red soild line), $\Upsilon = 1/3$ (blue dashed line), and $\Upsilon = 1/2$ (black dotted line) respectively.

The difference of two branches of decay rate from the excited state to the low-energy states is expressed as the normalized branch ratios Υ. The normalized branch ratio Υ is given by $\Upsilon = (\Gamma_{31} - \Gamma_{32})/(\Gamma_{31} + \Gamma_{31})$. $\Upsilon = 0$ corresponds to the balanced decay rates, on the contrary, $\Upsilon \neq 0$ corresponds to the unbalance decay rates. The more unbalanced the two branches of the decay rate are, the larger the value of Υ is. The precise calculation result of the frequency shift (FS) with respect to the normalized branch ratio Υ is shown in Fig. 2. For higher normalized branch ratios, the frequency shift of EIT (CPT) Ramsey processes will increase. Especially in the CPT-Ramsey shown in Fig. 2(b), when the two branches of the decay rate are no longer equal, the frequency shifts will be 15 times larger than the case of equalization. In the EIT-Ramsey shown in Fig. 2(a), the frequency shift slightly increases with the increase of the normalized branch ratio. In addition, when the two branches of decay rate are unbalanced, the frequency shift of EIT-Ramsey is an order of magnitude larger than that of CPT-Ramsey. The reason is that the unequal populations of low-energy states in EIT caused by two unequal Rabi frequencies result in a greater frequency shift. Therefore, in order to obtain a smaller frequency shift, it is necessary to control the decays of the excited state, especially for CPT-Ramsey process.

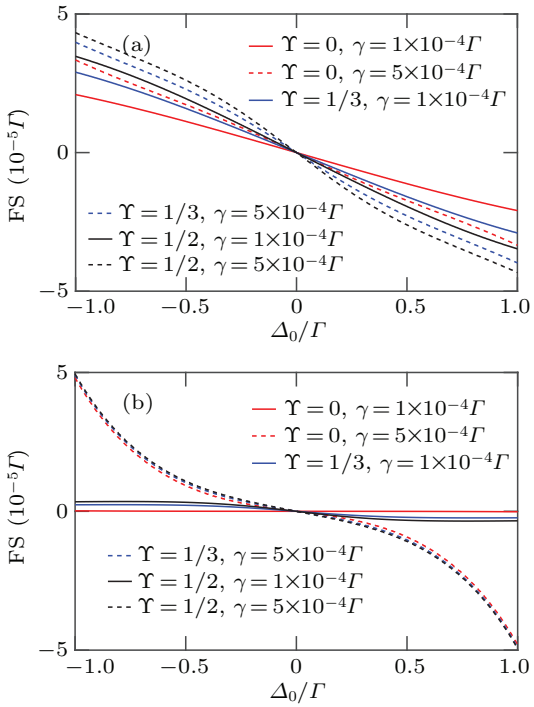

Fig. 3. (a) FSs of the center fringe of the EIT-Ramsey on the ρ_{33} excited state population vs. the common optical detuning Δ_0 with the different parameters Υ and γ. The Rabi frequencies are $\Omega_1 = 0.02\Gamma$ and $\Omega_2 = 0.005\Gamma$. The decay rates of the low energy states are $\gamma = 1 \times 10^{-4}\Gamma$ (soild line) and $\gamma = 5 \times 10^{-4}\Gamma$ (dashed line) respectively. The normalized branch ratios are $\Upsilon = 0$ (red line), $\Upsilon = 1/3$ (blue line), and $\Upsilon = 1/2$ (black line) respectively. (b) FSs of the center fringe of the CPT-Ramsey on the ρ_{33} excited state population vs. the common optical detuning Δ_0 with the different parameters Υ and γ. The Rabi frequencies are $\Omega_1 = \Omega_2 = 0.005\Gamma$. The decay rates of the low energy states are $\gamma = 1 \times 10^{-4}\Gamma$ (soild line) and $\gamma = 5 \times 10^{-4}\Gamma$ (dashed line) respectively. The normalized branch ratios are $\Upsilon = 0$ (red line), $\Upsilon = 1/3$ (blue line), and $\Upsilon = 1/2$ (black line) respectively.

The frequency shifts of the EIT (CPT)-Ramsey with respect to the normalized branch ratio Υ and the low-energy state relaxations γ are shown in Fig. 3. Different color lines in Fig. 3 represent different normalized branch ratios, and different kinds of lines represent the different relaxations of low-energy states. It can be clearly seen that frequency shifts in the two processes will increase with the increasing normalized branch ratios Υ and relaxations of low-energy states γ. However, there is a difference between the two processes. In the EIT-Ramsey shown in Fig. 3(a), the light shifts increase slightly with the increase of relaxations of the low-energy states γ and the normalized branch ratios Υ. In the CPT-Ramsey process shown in Fig. 3(b), the relaxations of the low-energy states γ affect the frequency shifts more seriously than the normalized branch ratio Υ. The main reason is that the

higher relaxations of the low-energy states can destroy the coherence of the low-energy states for the CPT-Ramsey, thereby causing a greater frequency shift. Therefore, the importance of controlling the relaxations of the low-energy states is far greater than controlling the decays of the excited state in the CPT-Ramsey.

For the different normalized branch ratio Υ and the Rabi frequency Ω_i ($i = 1, 2$), the variation of the frequency shift is shown in Fig. 4. It can be seen that whether it is EIT-Ramsey or CPT-Ramsey, the frequency shifts decrease as the Rabi frequencies increase. Under the pulse excitation, the physical picture of frequency shift is the residual coherence of the atomic states before the new coherent preparation. When higher light intensities are used, the frequency shift is reduced due to pulse saturation ($\Omega\tau \gg 1$). Comparing Fig. 4(a) with Fig. 4(b), it is found that the influence of the normalized branch ratio Υ on frequency shifts is slightly greater than Rabi frequency Ω_i in the EIT-Ramsey. But in the CPT-Ramsey, when the normalized branch ratio is not 0, the Rabi frequency has a stronger impact on the frequency shift.

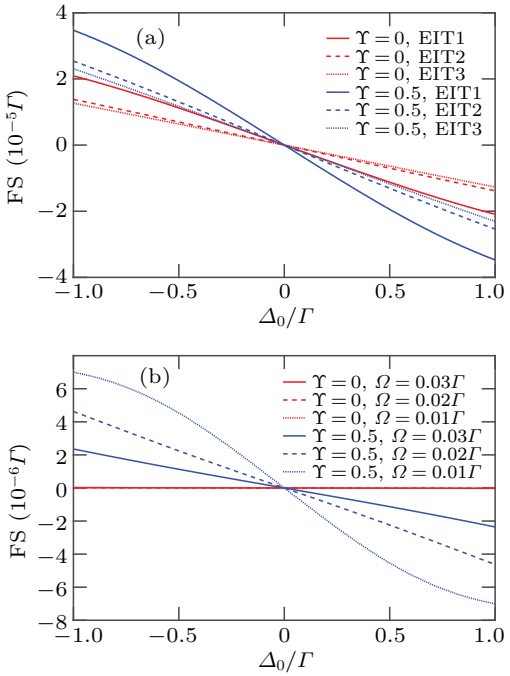

Fig. 4. (a) FSs of the center fringe of the EIT-Ramsey on the ρ_{33} excited state population vs. the common optical detuning Δ_0 with the different parameters Υ and Ω_i ($i = 1, 2$). The decay rates of the low energy states are $\gamma = 1 \times 10^{-4}\Gamma$. The normalized branch ratio are $\Upsilon = 0$ (red line) and $\Upsilon = 0.5$ (blue line) respectively. The Rabi frequencies in EIT1, EIT2, and EIT3 are $\Omega_1 = 0.02\Gamma, \Omega_2 = 0.005\Gamma$ (soild line), $\Omega_1 = 0.03\Gamma, \Omega_2 = 0.005\Gamma$ (dashed line), and $\Omega_1 = 0.03\Gamma, \Omega_2 = 0.0075\Gamma$ (dotted line), respectively. (b) FSs of the center fringe of the CPT-Ramsey on the ρ_{33} excited state population vs. the common optical detuning Δ_0 with the different parameters Υ and Ω_i ($i = 1, 2$). The decay rates of the low energy states are $\gamma = 1 \times 10^{-4}\Gamma$. The normalized branch ratios are $\Upsilon = 0$ (red line) and $\Upsilon = 0.5$ (blue line) respectively. The Rabi frequencies are $\Omega_1 = \Omega_2 = 0.03\Gamma$ (soild line), $\Omega_1 = \Omega_2 = 0.02\Gamma$ (dashed line), and $\Omega_1 = \Omega_2 = 0.01\Gamma$ (dotted line) respectively.

All these parameters Υ, γ, and Ω_i ($i = 1, 2$) affect the variations of the frequency shifts. But under the different processes, the influences of the three parameters on the frequency shifts are different. In order to more intuitively know how the frequency shifts are affected by the three parameters, we accurately calculated the frequency shifts of EIT (CPT)-Ramsey with the different parameters Υ, γ, Ω_i ($i = 1, 2$). The computed result is shown in Fig. 5. For the frequency shifts of EIT-Ramsey process shown in Fig. 5(a), the influence of the parameters Υ and γ on the frequency shifts is slightly larger than that of the parameter Ω_i ($i = 1, 2$). Consequently, the frequency shift corresponding to the green dashed line is much larger than that of the red dashed line. Therefore, in order to obtain a smaller frequency shift, the three parameters need to be adjusted respectively to obtain the most appropriate values. For the case of CPT-Ramsey shown in Fig. 5(b), γ has the greatest influence on the frequency shifts and it is much larger than the influence of other factors on the frequency shift. Therefore, in order to reduce frequency shifts in the CPT-Ramsey process, the relaxations of the low-energy states should be well controlled.

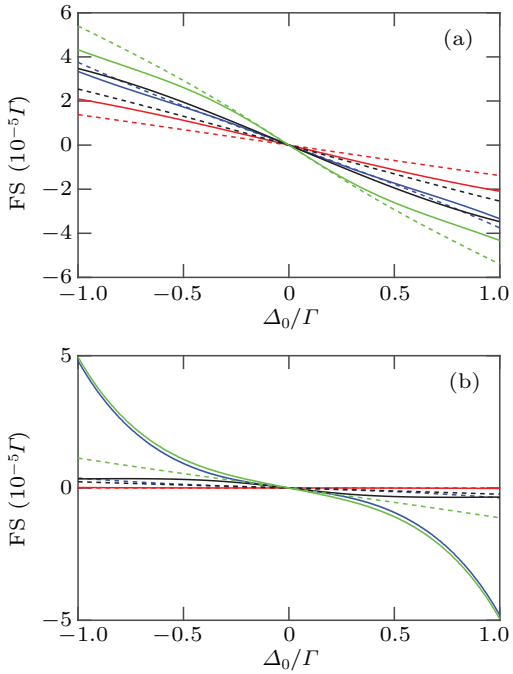

Fig. 5. (a) FSs of the center fringe of the EIT-Ramsey on the ρ_{33} excited state population vs. the common optical detuning Δ_0 with the different parameters Υ, γ, and Ω_i ($i = 1, 2$). The Rabi frequencies in EIT1 and EIT2 are $\Omega_1 = 0.02\Gamma, \Omega_2 = 0.005\Gamma$ (soild line) and $\Omega_1 = 0.03\Gamma, \Omega_2 = 0.005\Gamma$ (dashed line), respectively. The normalized branch ratio and the decay rates of the low energy states are $\Upsilon = 0, \gamma = 1 \times 10^{-4}\Gamma$ (red line), $\Upsilon = 0$, $\gamma = 5 \times 10^{-4}\Gamma$ (blue line), $\Upsilon = 0.5$, $\gamma = 1 \times 10^{-4}\Gamma$ (black line), $\Upsilon = 0.5$, and $\gamma = 5 \times 10^{-4}\Gamma$ (green line) respectively. (b) FSs of the center fringe of the CPT-Ramsey on the ρ_{33} excited state population vs. the common optical detuning Δ_0 with the different parameters Υ, γ, and Ω_i ($i = 1, 2$). The Rabi frequencies in CPT1 and CPT2 are $\Omega_1 = \Omega_2 = 0.005\Gamma$ (soild line) and $\Omega_1 = \Omega_2 = 0.03\Gamma$ (dashed line), respectively. The normalized branch ratios and the decay rates of the low energy states are $\Upsilon = 0$, $\gamma = 1 \times 10^{-4}\Gamma$ (red line), $\Upsilon = 0$, $\gamma = 5 \times 10^{-4}\Gamma$ (blue line), $\Upsilon = 0.5$, $\gamma = 1 \times 10^{-4}\Gamma$ (black line), and $\Upsilon = 0.5$, $\gamma = 5 \times 10^{-4}\Gamma$ (green line) respectively.

In conclusion, we accurately calculated the frequency shifts with the different parameters in the EIT (CPT)-Ramsey

pulse processes, such as the normalized branch ratio, the relaxation rates of the low-energy states, and the Rabi frequencies. The results show that the frequency shifts are closely related to these parameters. In both processes, the frequency shifts increase with the increases of the normalized branch ratio and relaxations of the low-energy states, and decrease with the increase of the Rabi frequency. The difference is that the influence of the normalized branch ratio and the relaxations of the low-energy states on frequency shifts is slightly larger than that of the Rabi frequency in the EIT-Ramsey process. However, in the CPT-Ramsey process, the frequency shifts are closely related to the relaxations of the low-energy states, which has a more significant influence on the frequency shifts than other parameters. Our research can be used for three-level atomic system of alkaline-earth metal atoms, such as ^{88}Sr atom. States $^1S_0$, $^3P_0$, and $^1P_1$ can form a three-level atomic system of ^{88}Sr atom. In such a system, the lasers drive the transition between states $^1S_0$ and $^1P_1$ and the transition between states $^3P_0$ and $^1P_1$.

References

[1] Vig J R 1993 *IEEE transactions on ultrasonics, ferroelectrics, and frequency control* **40** 522
[2] Arditi M and Carver T R 1963 *Proc. IEEE* **51** 190
[3] Marangos J P 1998 *J. Mod. Opt.* **45** 471
[4] Fleischhauer M, Imamoglu A and Marangos J P 2005 *Rev. Mod. Phys.* **77** 633
[5] Lukin M D 2003 *Rev. Mod. Phys.* **75** 457
[6] Scully M O and Zubairy M S 1999 *Quantum Optics* (Cambridge: Cambridge University Press) Chap. 7
[7] Arimondo E 1996 *Prog. Opt.* **35** 257
[8] Budker D and Kimball D F 2013 *Optical Magnetometry*
[9] Mescher M J, Lutwak R and Varghese M 2005 *TRANSDUCERS'05: 13th Int. Conf. on Solid-State Sensors, Actuators and Microsystems, Digest of Technical Papers* **1** 311
[10] Kitching J, Hollberg L, Knappe S and Wynands R 2011 *Electron. Lett.* **37** 1449
[11] Knappe S, Shah V, Schwindt P D D, Hollberg L, Kitching J, Liew L A and Moreland J 2004 *Appl. Phys. Lett.* **85** 1460
[12] Zanon T, Guerandel S, de Clercq E, Holleville D, Dimarcq N and Clairon A 2005 *Phys. Rev. Lett.* **94** 193002
[13] Kozlova O, Danet J M, Guérandel S and de Clercq E 2014 *IEEE Trans. Instrum. Meas.* **63** 1863
[14] Kotru K, Brown J M, Butts D L, Kinast J M and Stoner R E 2016 *Phy. Rev. A* **90** 053611
[15] Esnault F X, Blanshan E, Ivanov E N, Scholten R E, Kitching J and Donley E A 2013 *Phys. Rev. A* **88** 042120
[16] Zanon-Willette T, Ludlow A D, Blatt S, Boyd M M, Arimondo E and Ye J 2006 *Phys. Rev. Lett.* **97** 233001
[17] Zanon-Willette T, de Clercq E and Arimondo E 2011 *Phys. Rev. A* **84** 062502
[18] Pati G S, Fatemi F K, Bashkansky M and Shahriar S 2010 *Proc. SPIE* **7949** 794910
[19] Yano Y, Gao W J and Goka S 2014 *Phys. Rev. A* **90** 013826
[20] Liu X, Merolla J M, Guerandel S, de Clercq E and Boudot R 2013 *Opt. Express* **21** 12451
[21] Talchenachev A V, Yudin V I, Wynands R, Stahler M, Kitching J and Hollberg L 2003 *Phys. Rev. A* **67** 033810
[22] Pati G S, Warren Z, Yu N and Shahriar M S 2015 *J. Opt. Soc. Am. B* **32** 388
[23] Zanon T, Tremine S, Guerandel S, de Clercq E, Holleville D, Dimarcq N and Clairon A 2005 *Instrum. Meas.* **54** 776
[24] Hemmer P R, Shahriar M S, Natoli V D and Ezekiel S 1989 *J. Opt. Soc. Am. B* **6** 1519